

AD-A101 401 FOREIGN TECHNOLOGY DIV WRIGHT-PATTERSON AFB OH
AN ANALYSIS OF HIGH-POWER RADAR TR-LIMITED WITH VERY SHORT RECO--ETC(U)
MAY 81 J HSU, C TONG
UNCLASSIFIED FTD-ID(RS)T-1903-80

F/6 9/1

NL

1 of 1
A-0420

END
DATE
FILED
8-88N
DTIC

(2)

FTD-ID(RS)T-1903-80

ADA101401

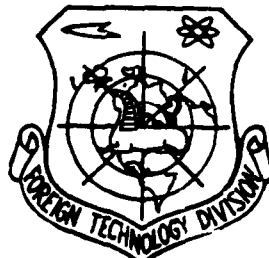
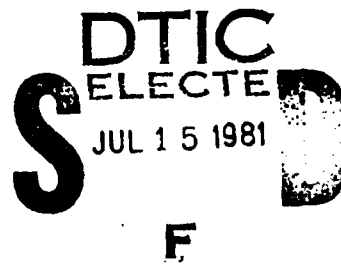
FOREIGN TECHNOLOGY DIVISION



AN ANALYSIS OF HIGH-POWER RADAR TR-LIMITED
WITH VERY SHORT RECOVERY TIME

by

Hsu Jun-min and Tong Cin-Shian



Approved for public release;
distribution unlimited.

DTIC FILE COPY

FTD-ID(RS)T-1903-80

EDITED TRANSLATION

FTD-ID(RS)T-1903-80

7 May 1981

MICROFICHE NR: FTD-81-C-000402

AN ANALYSIS OF HIGH-POWER RADAR TR-LIMITED
WITH VERY SHORT RECOVERY TIME

By: Hsu Jun-min ~~Hsu~~ Tong Cin-Shian ~~/1981~~

English pages: 43

Sichuan Daxue Xuebao, Ziran Kexue,
Vol. 3, 1979, pp. 79-81, 84-100
pages 82 and 83 missing in original
foreign document 1979.

Country of origin: China

Translated: SCITRAN

F33657-78-D-0619

Requester: FTD/TQTA

Approved for public release; distribution
unlimited.

Accession For	
PTIG GRA&I	
DTIG TAB	
Unclassified	
Justification	
Py.	
Distribution/	
Availability Codes	
Avail and/or	
Distr	Special
A	

THIS TRANSLATION IS A RENDITION OF THE ORIGINAL FOREIGN TEXT WITHOUT ANY ANALYTICAL OR EDITORIAL COMMENT. STATEMENTS OR THEORIES ADVOCATED OR IMPLIED ARE THOSE OF THE SOURCE AND DO NOT NECESSARILY REFLECT THE POSITION OR OPINION OF THE FOREIGN TECHNOLOGY DIVISION.

PREPARED BY:

TRANSLATION DIVISION
FOREIGN TECHNOLOGY DIVISION
WP-AFB, OHIO.

FTD-ID(RS)T-1903-80

Date 7 May 1981

141600

AN ANALYSIS OF HIGH-POWER RADAR TR-LIMITER WITH VERY
SHORT RECOVERY TIME

Hsu Jun-min and Tong Cin-Shian

Preface

There have been three basic techniques employed in the design of protectors for radar receivers in the past; these are plasma, ferrites, and semiconducting diodes. Some people [i] have already made more comprehensive, detailed discourses about the protection capabilities and other characteristics afforded the radars by the TR limiters designed according to these techniques. However, let us consider the pulse doppler radars. Since such a radar has higher pulse repetition frequency (PRF), then the protection for its receiver will not only require lower insertion loss and the capability to handle high power but also its recovery time τ_B must be extremely short. Normally, it is required that

$$\tau_B < \frac{\tau}{3}$$

where τ is the transmitting pulse width. Therefore, if we utilize any single one of the above techniques the TR limiter cannot satisfy the requirements of a pulse doppler radar. However, combining the above techniques and improving the combination, as for example in a ferrite-diode limiter, or a gas plasma-diode limiter, and the currently available electronic multiplier limiter, have contributed some paths to solution of the problems in the pulse doppler radars. We give some introduction to these three TR limiters in the following sections. We shall specifically make further theoretical analysis, in this paper, of electronic multiplier limiters.

1. Ferrite-diode limiter

This is a combination of a ferrite limiter and a diode limiter. We know that although a pure ferrite limiter has

large capacity for power, its spike and flat leakages are large, so it cannot protect an agile receiver. A pure diode semiconducting diode limiter has small power capacity and is not adequate for high power applications. However, either one of these, be it ferrite limiter or diode limiter, has extremely short recovery time, about tens of nanoseconds. Therefore, when we combine their capabilities we have a limiter that would possess two important characteristics: tolerance for high power and extremely short recovery time. Then it is possible to apply such a limiter to pulse doppler radars. Within this combination the ferrite limiter reduces the large radio frequency (RF) input power to the voltage level that can be tolerated by the semiconducting diode. Then the semiconducting diode serves to inhibit the flat and peak leakages coming from the ferrite limiter, thereby achieving the voltage that can be tolerated by the receiver.

- In the following we make some simple descriptions of the structure and capabilities of two ferrite-diode limiters that have been reported abroad [2, 3].

1. Ferrite limiter

The working principle of a ferrite limiter is based on the nonlinear effect of high power on ferrite. In order to achieve a usable bandwidth greater than 1% we must apply the subsidiary-resonance limit of the nonlinear effect (the one-time effect). [4]

In the ferromagnetic resonance with the high frequency region that continuously increases to a certain value, there appears a phenomenon of a premature saturation of the primary peak, and a subsidiary absorption peak. The aforementioned value of the high frequency region is called the near threshold

region, h_c , as shown in Figure 1.1.

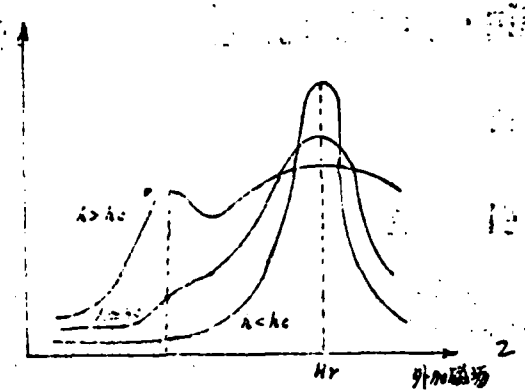


Figure 1.1. Primary peak saturation and subsidiary absorption peak phenomenon.

1. Relative power absorption, 2. externally added (induced) magnetic field.

Theoretical analysis has indicated that the appearance of an absorption peak is the result of a coupling effect of spin-wave and an accompanying amplitude. Also, when the frequency ω_k has the value of one-half ω , the frequency of the externally induced high frequency region, it is easiest to excite the spin-waves. Since $\omega_k = 1/2 \omega < \omega$, the primary resonance absorption frequency and the additional absorption peaks will appear in places lower than the primary peaks.

In order to lower the threshold power of the ferrite limiter we find the applications of lamination structure and horizontal biasing (magnetic) field techniques to be superior.

(1) Lamination structure

We may use the same method which is used to reduce the near threshold region to lower the threshold power of a ferrite limiter. Under the situation of the subsidiary

resonance limiting, the limiting threshold region is not only related to the material characteristics, but also to the geometric configuration of the samples (targets). The latter is related to the appearance of the shape of the demagnetization factor in the limiting threshold region. The computations and analyses of the references have indicated that when a magnetic biasing field is placed in the direction with the smallest demagnetic agent, the smallest near threshold region will be obtained. Therefore, in the usual structure one needs a very long ferrite rod and applies the magnetic biasing field along the longitudinal axis. However, this structure brings in two serious disadvantages. One of them is that the magnetic biasing field can be obtained only by the use of a solenoid or a large, heavy permanent magnet. The other is that only a small amount of microwave interaction can be obtained because of the low waveguide filling factors.

An alternative to using the method mentioned above is to place the long axis of the ferrite rod along the narrow dimension of the waveguide and apply the magnetic biasing field along this axis. Even though this guarantees that the magnetic biasing field is applied in that direction possessing the smallest demagnetization factor, since the cross-section of the ferrite rod must be small in comparison to its length, it can only utilize ferrite material with very small (body) volume, which results in an inadequate dynamic range of the limiter. However, this can be overcome by the following method. Place a large number of rectangular ferrite rods along the longitudinal axis of the waveguide, and separate them by dielectric rods of the same dimensions and dielectric constant (as the ferrite rods). This device is called a laminar structure. The dielectric rods provide magnetic insulation between the ferrite rods, so that the bias of each ferrite rod is independent, thereby maintaining its own demagnetization factor. Simultaneously

the dielectric rods have an effect of resistance. The X-band laminar structure is shown in Figure 1.2. The laminar structure employs six polycrystalline YIG rods. This kind of structure has characteristics of low insertion loss and high power limiting, as illustrated in Figures 1.3 and 1.4.

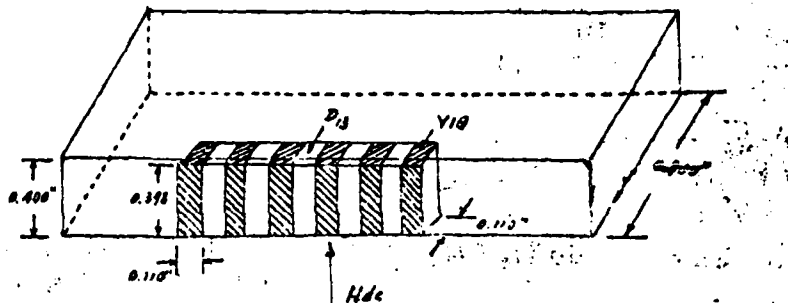


Figure 1.2. X-band laminar limiter structure.

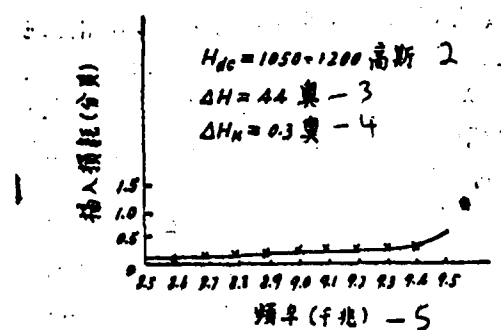


Figure 1.3. Low-level insertion loss versus frequency (for six polycrystalline YIG rods) in the laminar structure.
 1. Insertion loss (dB), 2. $\Delta H_{dc} = (1050 \text{ to } 1200 \text{ gauss})$, 3. $\Delta H = 44 \text{ Oe}$; 4- $\Delta H_K = 0.3 \text{ Oe}$, 5. Frequency (GHz).

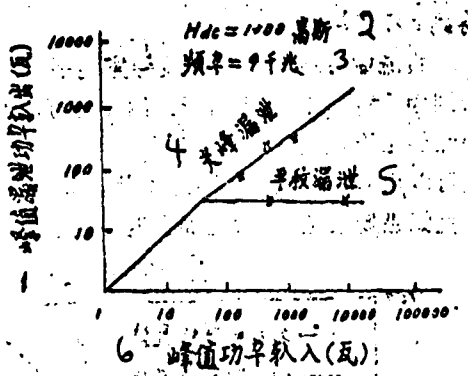


Figure 1.4. High-power characteristics for the laminar structure.

1. peak leakage power output (watts), 2. $H_{dc} = 1000$ gauss;
3. frequency - 9 GHz, 4. spike leakage; 5. flat leakage;
6. peak power input (watts).

We can see that within 8% of the frequency range the maximum insertion loss of this kind of structure is 0.6 dB. It is superior when compared with other subsidiary resonance limiters; its limiting threshold power is 28 watts, and the dynamic range for the flat attenuation is 23 dB. This is indeed the direction of the minimum demagnetization factor in which we place the biasing magnetic field (within this structure); thus we obtained a limiting threshold power lower than the usual subsidiary resonance limiters. Also, selecting the laminar structure guarantees a sufficient volume of the ferrite material, thereby obtaining such good limiter dynamic range.

Further experiments indicate that if we adopt an inclined biasing magnetic field at an angle of 30 degrees from the vertical direction, then the laminar structure can increase its flat and spike limiting power. It is still a difficult task to make a detailed analysis under this condition. Qualitatively speaking, the reduction of the limiting threshold power and the increasing of spike inhibition suggests the high degree of concentration in the ferrite magnetic field and

the appearance of an extra quantity of the transmitting frequency magnetic field. This extra quantity is produced by the interaction of the horizontal component of the biasing magnetic field and the longitudinal component of the transmitting frequency range.

The subsidiary resonance limiter of laminar structure, if it is like any ferrite limiter, has larger spike leakage. The spike leakage pulse has a 3 dB width of about 30 ns. The peak spike power is about 3 kW for an input power of 10 kW. Therefore, in order to have a usable (TR) limiter, we must connect a diode limiter behind it to inhibit this large spike leakage. However, since a laminar structure has a lower limiting threshold power, this may utilize diode limiters of lower power, or it may raise the fixed power of a ferrite-diode limiter combination.

(2) Horizontally biased ferrite limiter

Its fundamental structure is as illustrated in Figure 1.5. The ferrite elements completely fill the rectangular waveguides of the compressed cross-section. The four long sides of the ferrites are metallized and are welded to the walls of the waveguides. As for the X-band limiters, the ferrite and waveguide cross-sections are $0.19 \times 0.375 \text{ in}^2$ or $0.19 \times 0.500 \text{ in}^2$. The ferrite material used is polycrystalline YIG, and its characteristics are: saturation magnetization intensity of the material ($4\pi M_s$) is 1780 gauss, uniform precessional linewidth (ΔH) is 45 Oe, the dielectric constant (ϵ) is 15, the tangential medium loss is less than 0.002, and the spin-wave linewidth (ΔH_K) is 1.4 Oe.

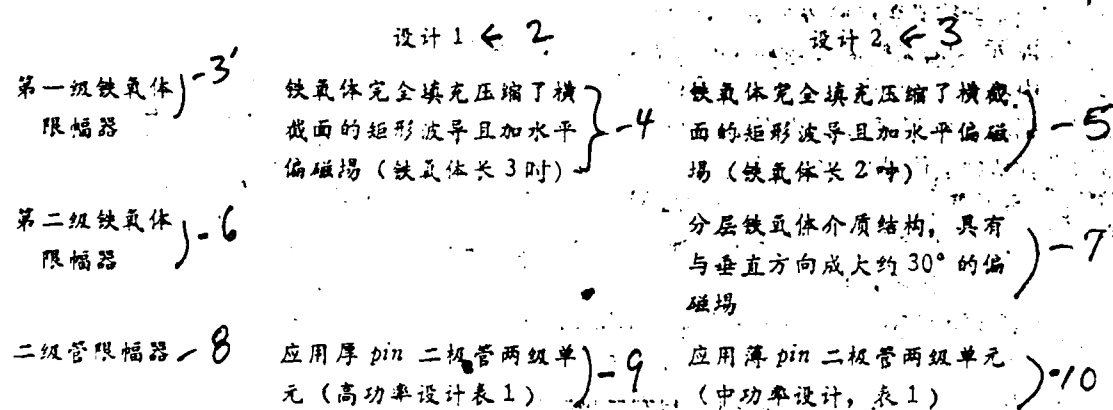
Translator's note: I regret to say that this is the end of p. 81 of the original (foreign) manuscript, and pp. 82-83 have not been supplied. The best thing that I can do is to pick up from the beginning of p. 84, which happens to be the beginning of a new paragraph, and that Table 2 of p. 84 is about X-band ferrite-diode limiter characteristics; seems to be a good place to continue.

The following starts with the beginning of p. 84.

The second kind of structure is a combination of the aforementioned high-power-class ferrite limiter (ferrite rod length of 2 inches), inclined magnetic biasing field laminar medium power ferrite limiter and medium power diode limiter. This combination has a total insertion loss of 1.5 dB. When the input power reaches 100 kW the maximum flat leakage and the spike leakage are respectively 14 and 70 milliwatt (at 0.01 erg).

Table 2 lists the important characteristics of the ferrite-diode limiter.

Table 2. Characteristics of an X-band ferrite diode limiter



性能	— 11
峰值功率 (千瓦)	— 12 100
平均功率 (瓦)	— 13 100
脉冲宽度 (微秒)	— 14 5
插入损耗 (分贝)	— 15 1.3
带 宽 (%)	— 16 5~8
最大平坦漏泄 (毫瓦)	— 17 18
尖峰漏泄幅度 (毫瓦)	— 18 800
尖峰漏泄能量 (尔格)	— 19 0.1
恢复时间 (毫微秒)	— 20 50

Key:

2. Design #1
3. Design #2
- 3'. First stage ferrite limiter
4. Ferrite completely filled the rectangular waveguide of the reduced cross-section, with horizontal biasing magnetic field (ferrite length is 3").
5. Ferrite completely filled the rectangular waveguide of the reduced cross section, with horizontal biasing magnetic field (ferrite length is 2").
6. Second stage ferrite limiter.
7. Laminar ferrite dielectric structure with magnetic biasing field at approximately 30° with respect to the vertical direction.
8. Diode limiter.
9. Two-stage unit utilizing thick PIN diode (high-power design, see Table 1).
10. Two-stage unit utilizing thin PIN diode (medium power design, see Table 1).
11. Capability and characteristics.
12. Peak power (KW).
13. Average power (W).
14. Pulse width (μs).
15. Insertion loss (dB).
16. Bandwidth (%).
17. Maximum flat leakage (mW).
18. Spike amplitude leakage (mW).
19. Spike energy leakage (ergs).
20. Recovery time (ns)

We can see from the table that a ferrite-diode limiter can satisfy the high power requirements of pulse doppler radars, i.e. tolerance for high power and very short recovery time. However, its insertion loss is large, and also it is both bulky and heavy. This is primarily caused by requirements of using long ferrite rods to achieve sufficiently large dynamic range. Reference [5] suggests a new structure of multilayer ferrite limiter. This is formed by interleaving four Al-300 dielectric slabs with four slabs of YIG ferrite, placed on the narrow wall of a reduced-height and reduced-width rectangular wave guide. The thicknesses of the ferrite and dielectric slabs are selected experimentally to achieve the maximum dynamic range. However, the ferrite slabs are only 1.5 in. long. In the 5.4 - 5.9 GHz frequency band region,

this multilayer limiter has a (below the threshold) insertion loss of less than 0.5 dB, the threshold power is about 20W and the dynamic range is greater than 200 kW. However, for a single layer ferrite limiter to achieve the same dynamic range its slab length needs to be 7 in. long. Therefore, there is still potency in the reduction of the volume of ferrite-diode limiter.

§ 2 Plasma diode limiter

Everyone knows that the early TR tubes (devices) had a serious number of deficiencies, e.g. large noise, short operating life span, low reliability, and long recovery time. There are two principal reasons for these, one of them being the need for an ignition voltage (arc protection), or receiver protector (keep alive), the device thereby being a noise generator. The other is caused by the glass discharge window and discharge electrode absorption gases which make the gas pressure (density) inside the tube (device) to be lowered, and also the electrode can be easily damaged while discharging.

In order to overcome the above deficiencies, people had, during the 1960's, used a radioactive source (tritium) to replace the active arc (receiver) protector (keep alive) within the TR tube(s). However, since the radioactive ignitor-supplied free electron density is much lower than that supplied by the dc-arc protector, this leads to an increase in ignition threshold and spike leakage. Therefore, we must attach a single stage or dual stage diode limiter. From this, we have the widely used passive TR limiter. However, although its recovery time is shorter than the active TR tubes, it still cannot satisfy the requirements of the high repetition frequency of pulse doppler radars.

In order to further shorten the recovery time of TR tubes we must quickly eliminate the free electrons in the discharger after the end of the transmitting pulse. We may hereby utilize the neutralization of the negative ion iteration.

We hope to utilize the comparatively conductive electronegative gases. Within these gases, due to the fact that electrons are attracted to neutral molecules or neutral atoms forming the negative ions, halogen gas has the required property. However, in order to lower the electric arc leakage power (an important part of flat leakage), the gas must have the smallest discharge maintenance voltage of ultra-high frequency, and it also requires single atom gas of very small conductivity, e.g., inert gas. Therefore, in order to shorten the recovery time we need to use ~~a~~ large volume of conducting inert gas and a small volume of conducting gas to reduce arc leakage.

Past solution to this contradiction was done with a compromise. This can be done by filling the TR tubes with inert gases containing electronegative impurities. The recovery time is more than 1 ms. Then it is still difficult to satisfy the requirements of the pulse doppler radars.

Reference [6] reported a kind of separation stage design that is better in solving the aforementioned contradiction, thereby obtaining a very short recovery time. It is illustrated in Figure 2.1. That is, it is composed of three separation stages: high power stage, medium power stage, and diode limiter. The discharger is filled with a halogen to obtain short recovery time.

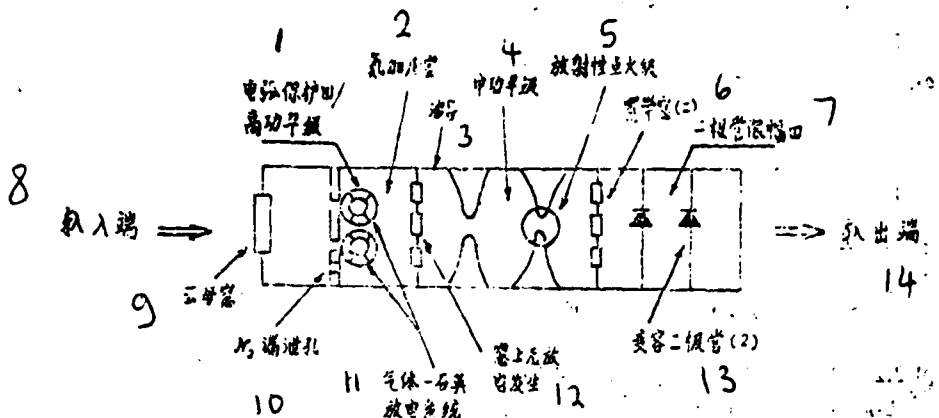


图 2.1 — 15

Figure 2.1.

Key: 1. High power stage arc (receiver protector), 2. N_2 backfill, 3. wave guide, 4. medium power stage, 5. radioactive ignition stage, 6. wideband window (two), 7. diode limiter, 8. input interface, 9. rexolite pressure window, 10. N_2 leakage hole (valve), 11. gas-quartz discharge system, 12. there is no discharge on these windows, 13. thin PIN diode, 14. output interface, 15. Figure 2.1.

The high power stage discharging system is composed of halogen gas-filled quartz bubbles. In order to increase the power capacity we may place a number of quartz bubbles in the plane. This will increase the internal pressure on the waveguides surrounding the quartz bubbles thereby improving the reliability. This is the reason for using rexolite windows at the input portion and the output portion (of the high power stage), that is, the input portion of the medium power stage uses wideband windows, thus forming a hermetically sealed external shell to increase pressure on the N_2 backfill. The rexolite used on the input window was chosen because of its resistance to high temperature, but if glass were used here it would explode, or soften, rendering it useless. Also, after passing such a tight seal it can still

avoid steam, dust and other contaminants, to maintain a high Q opening. The external pressurized N₂-filled rexolite shell and its surrounding metal circular ring can thereby prevent sparking, corrosion, and rusting.

The utility of the medium power stage is to reduce the power which leaks through the high power stage to the range that can be tolerated by the diode limiter. It is a common TR discharger with radioactive ignitor. The differences are that their input and output windows are wideband, thus the window will not discharge. This solves the problem of the discharge window absorbing gas molecules thereby lowering the gas pressure of the discharger, which will shorten the operating life. So, this kind of structure will clearly lengthen the operating life of the system.

The lower power stage is indeed a semiconducting diode limiter; its utility is to reduce the power leaking through the medium power stage to a level tolerable by the capacity of the receiver.

The X-band plasma-diode limiter leakage amplitude and recovery time as functions of input power are plotted in Figures 2.2, 2.3 and 2.4. When the spike and flat leakage amplitudes are within 10% of the frequency band, the direct input power of 10 kW are respectively less than 50 and 20 mW. At 3 dB the recovery time in the range of 100 W to 50 kW is less than 140 ns. We can see from the figure that when input power is greater than the quartz bubble threshold power, i.e. in the range of 0.1 to 10 kW, the leakage is small and the recovery time is always short and their values are stable. Obviously this is due to the fact that there are no window discharges. In the pulse doppler radar where the inter-pulse stability is very important, the plasma-

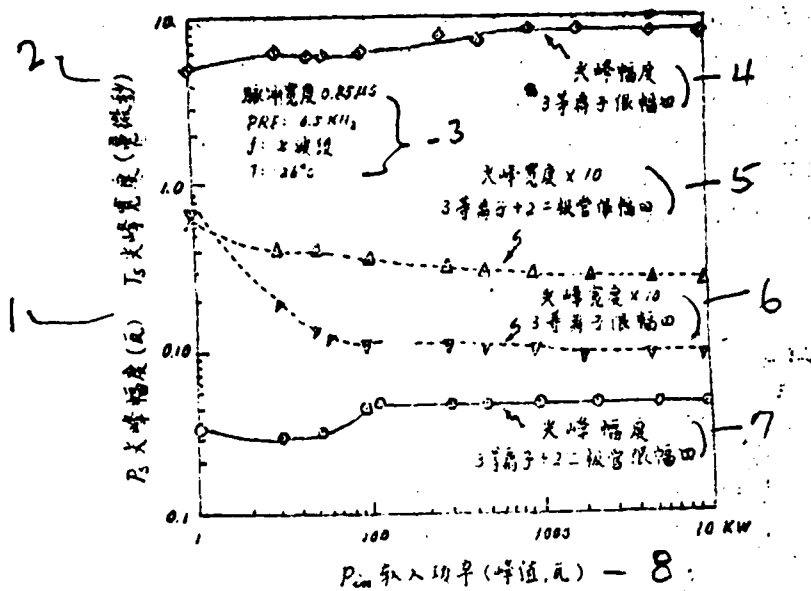


Figure 2.2. The addition of diode limiters has caused the spike amplitude to rapidly decrease, and the spike width to increase. However, the spike capacity can be kept under 0.005 erg, under all voltage power.

Key: 1. P_s spike amplitude (watts); 2. T_s spike widths (ns),
 3. pulse width 0.85 μ s, PRF: 0.5 KHz, f: X-band, T: 26°C
 (could have been -26°C, but the reproduction is very poor),
 4. spike amplitude, 3 plasma limiters, 5. spike width X10,
 3 plasma plus 2 diode limiters, 6. spike width X10, 3 plasma
 limiters, 7. spike amplitude, 3 plasmas plus 2 diode limiters,
 8. PIN input power (spike in watts).

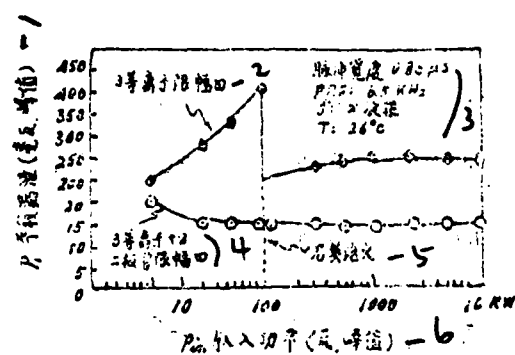


Figure 2.3. The introduction of diode limiters has flattened the flat leakage characteristics in the 30 dB range of the incident radiation power.

Key: 1. P_1 flat leakage (watt); 2. 3 plasma limiters, 3. pulse width = 0.85 μ s, PRF: 6.5 KHz, f: X-band, T: 26°C; 4. 3 plasma plus 2 diode limiters, 5. quartz ignition, 6. PIN input power (watts).

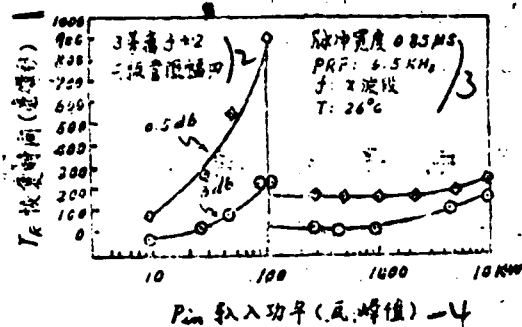


Figure 2.4. Recovery time, at 3 dB, is 250 ns for up to 10kW.

Key: 1. T_R recovery time (ns); 2. 3 plasma plus 2 diode limiters; 3. pulse width = 0.85 μ s, PRF: 6.5 KHz, f: X-band, T: 26°C; 4. PIN input power (watts).

diode limiter possessing stable recovery time, in the range of very large input power, has a very important implication. Under an average power of 200W the experiments on operating life spans have indicated that during 5,600 hours of operation the device leakage, recovery time, and insertion loss characteristics have not significantly degraded. This implies that plasma-diode limiter may possess operating life in excess of 10,000 hours of transmission.

The various (electrical) parameters of the C-band, S-band, and L-band plasma-diode limiters are given in Table 3. It can be seen in the table that this kind of limiter possesses not only the capability to handle high power and have low insertion loss, but also has rather short recovery time. They can be applied in the pulse doppler radars. Besides, they do not need an extra energy (power) source, therefore they serve to protect the receiver during the radar switching periods; that is, they may still protect (the receiver) during the asynchronous pulse period of the nuclear blast phenomenon. This has very important implications in modern warfare.

Table 3. Plasma-diode limiter's greatest
(most important) electric characteristics

① - 参 壮	WD-132	WD-191	WD-160	WD-242A	WD-356
	(S 波段)	(C 波段)	(X 波段)	(X 波段)	(L 波段)
入射功率-7 (kW)	0-100	0-70	0-0.5	0-10	0-500
插入损耗-8 (db)	0.6	0.7	0.7	0.8	0.6
插入相位偏差-9 差(度)	10	8	8	10	N/A
带宽-10 (%)	8%	12%	10%	10%	7%
温度范围-11 (°C)	← -50° — +80 °C →				
占空因数-12	0.04	0.006	0.5	0.01	0.006
尖峰漏泄能 量(尔格)-13	0.05	0.05	0.05	0.05	0.008
尖峰幅度 (MW 峰值)-14	400	250	500	50	30
平稳漏泄 (MW 峰值)-15	25	15	25	20	5
3db 恢复时 间(微秒)-16	0.35	20	0.15	0.4	10
射频工作寿 命(小时)-17	>10000	>10000	>10000	>10000	20000
保护对象-18	参放+混 频器	场效应晶 体管	参放+混 频器	参放+混 频器	双极性晶体 管放大器
	19	20	21	22	23

1. Parameter; 2. S-band; 3, C-band; 4. X-band; 5. X-band;
6. L-band; 7. incident radiation power (kW); 8. insertion
loss (dB), 9. insertion phase in bias (degree), 10. band-
width (%); 11. temperature (°C); 12. filler factor; 13.
spike leakage capacity (erg); 14. spike amplitude (MW); 15.
flat leakage (MW); 16. 3 dB recovery time (μs); 17. transmitter
operating life (hours); 18, object of protection; 19. radio-
active plus frequency mixer; 20. field effect transistor;
21, radioactive plus frequency mixer; 22. radioactive plus
frequency mixer; 23. bipolar transistor amplifier.

§ 3 Electronic Multiplier limiter (or multipactor limiter)

The electronic multiplier limiter is a new device, and it was first utilized in the doppler radar of the American AWACS system. It has been discussed very briefly in reference [7]. It may still be classified. We make an introduction and analysis of the principles of applications and characteristics of this device in the following.

1. The physical process of the multiple multipactor

In most of the low pressure environment, under the medium to high voltage RF capacity, electrons are used in the RF field to bombard the surfaces of a solid to cause secondary electronic emission. Pulse secondary electrons will absorb energy of the RF field, and they will bombard some other surfaces, producing more secondary electrons. This is the multipacting (multiple impacting) process. Since the electrons continuously absorb energy of the RF field in this process, they produce the limiting effect. This is called the multiple multiplier limiting effect (or multipacting). Clearly, in most electronic devices one usually avoids this kind of effect. Therefore, there were people who studied this effect much earlier and had predicted that it might gain applications in some RF devices. [8]

The electronic multipactor limiter is constructed from the aforementioned effect. The electronic multipactor limiter working principle is shown in Figure 3.1. There is a ridge in the inside wall of the two wide sides of the rectangular waveguides, and a constant gap is maintained between the ridge surfaces. The flat surfaces are to be coated with secondary material such as magnesium oxide (MgO), thus forming

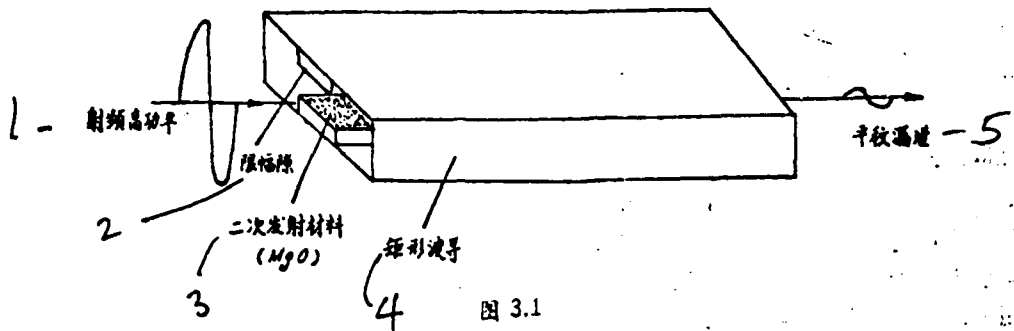


Figure 3.1.

Key: 1. high power RF, 2. limiting gap, 3. secondary emission material (MgO), 4. rectangular waveguide, 5. flat leakage.

the limiting gap. There is an electronic gun attached to the gap for injecting the electrons while the limiter is operating. The entire limiting gap and the electronic gun are tightly sealed in a vacuum system. When the RF power enters the limiter, the high frequency field built on the gap will force the primary electrons to traverse the gap to bombard the coated surface, causing emission of the secondary electrons. If the time that it takes the electrons to traverse the gap is equal to one half of the period of the changes in the high frequency field then the secondary electrons will be accelerated by the high frequency field to bombard another coated surface, thereby producing more secondary electrons. The electrons and the high frequency field will continuously interact in this manner. If the coefficient of the secondary emission of the coated surface is greater than 1 then the resultant secondary electrons will continue to multiply, and the gap will quickly have very high density of electrons. As the number of electrons increases in the gap, the (electric) charge field in the gap will continuously grow stronger, until the space charge field cancels the accelerating effect of

the high frequency field on the secondary electrons; this has built the final equilibrium status. At this time, the number of electrons on the bombarding surface is equal to that of the emitting secondary electrons, which were induced by the bombardment. The density of electrons in the gap continues to rise, and the electron cloud moves in the same direction as the externally added RF field. This electron cloud absorbs energy from the RF field, from which a limiting effect is produced. The energy not absorbed is transmitted as flat leakage.

According to the space kinetic equation of the free electrons being affected by the high frequency (electric) field and the condition of the traverse time of the electrons being equal to one-half of the high frequency period, reference [7] has contained the information about the required synchronous voltage V_0 for triggering the electronic multipacting process. Taking into account the corresponding input power threshold valve P_c , we have the following equations:

$$V_0 = 4\pi d^2 f^2 / \eta \quad (3.1)$$

$$P_c = 8\epsilon_0 W V_0 g d^3 f^4 / \eta^2 \quad (3.2)$$

where d is the width of the gap (or the resonator gap)

f is the frequency of the incoming RF wave

η is the specific electronic charge (i.e. electron charge - mass ratio)

ϵ_0 is the dielectric constant of the vacuum (i.e. permitivity of free space)

W is the width of the ridge of the waveguide

V_g is the corresponding velocity of the wave inside the gap (i.e. phase velocity of the RF wave)

The threshold power is the least of the input power in the process of triggering the electronic multipacting. When the input power is less than the threshold power the traverse time of the electrons in the gap will exceed one-half of the period of the high frequency field, and the synchronous condition cannot be satisfied. Therefore, the electronic multipacting process cannot be triggered. When the input power is greater than the threshold power, even if the traverse time of the electrons in the gap is less than one-half of the period of the high frequency, the electronic multipacting process can still be triggered. We believe that this is due to the fact that the secondary emission material, magnesium oxide, possesses self-sustaining emission characteristics, and that when the input power exceeds the threshold power these characteristics help to trigger the electronic multipacting. Under the condition when input power is greater than threshold power, due to the fact that electron traverse time is less than one-half of the period (of the high frequency field), even ^{for} the primary electrons bombarding the boundary surface of the limiting gap, the high frequency electric field is unable to react instantly, ~~but~~ after the high frequency field has reacted, the bombarded surface will emit secondary electrons. Therefore, the movement of the electronic cloud in the gap can still be synchronously in phase with the high frequency field.

Other reasons for using magnesium oxide as secondary emission material are: it can supply high current density, it can tolerate higher temperature, and it is more stable even when it is exposed to air for a time without suffering any ill effect.

2. An analysis of the structure of the electronic multipacting limiter.

The main part of the electronic multipacting limiter is put inside the limiting gap of the rectangular waveguide, and the two surfaces of the gap which face each other are coated with the magnesium oxide secondary emitting material. In order to dissipate heat, the limiting gap is hollow to permit flow of coolant, as shown in Figure 3.2. In the space between the limiting gap and the standard waveguide we should connect a damping device. In order to maintain the appropriate vacuum of the limiting gap, the input and output ends should be hermetically sealed with resonance windows, and the side window of the waveguide serves as a conduit for an ion pump. Besides serving the purpose of sealers the resonance windows also have the effect of filtering the waves. Therefore, any signals external to the band received by the antenna will be reflected and are absorbed by the terminal No. 4 of the ring shaped device as shown in Figure 3.3. The initial primary electrons, required by the multipacting process, are supplied by a small electron gun, which does not have stringent requirements. The electron gun is situated near the narrow side of the waveguide of the limiting gap. In the multipacting process some of the magnesium oxide secondary emission material, after being bombarded by electrons, is transformed into the state of basic magnesium metal. In order to oxidize this metal again the electronic multipacting limiter will have in it an oxygen generator.

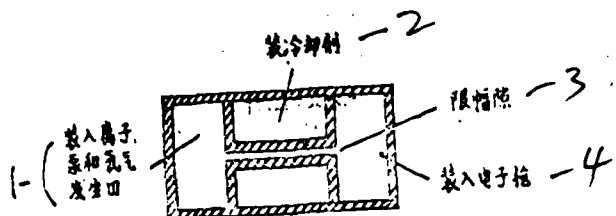


Figure 3.2.

Key: 1. install here an ion pump and an oxygen generator;
2. fill in coolant; 3. limiting gap; 4. install electron gun here.

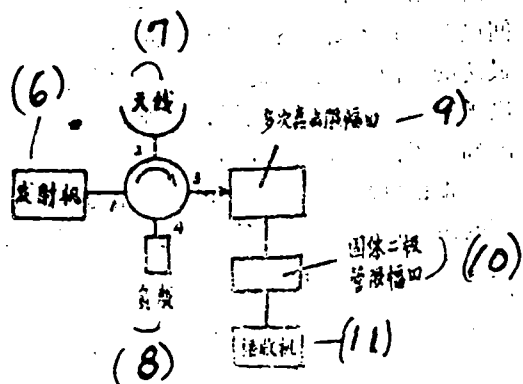


Figure 3.3.

6. emitter; 7. antenna; 8. load, 9. repeating bombardment limiter, 10. solid diode limiter, 11. receiver.

Furthermore, assuring the mechanical precision of the limiting gap distance is a monumental technical problem. The theoretically designed value of the limiting gap distance is d and, due to the manufacturing tolerance its actual value is $d + \Delta d$. Then the threshold power is changed from P_c to P_c' , and according to equation (3.2), we have

$$\begin{aligned}
 P_c' &= 8\epsilon_0 W V g (d + \Delta d)^3 f^4 / \eta^2 \\
 &= (8\epsilon_0 W V g d^3 f^4 / \eta^2) \left(1 + \frac{3\Delta d}{d} + \frac{3\Delta d^2}{d^2} + \frac{\Delta d^3}{d^3}\right) \\
 &\approx P_c \left(1 + \frac{3\Delta d}{d} + \frac{3\Delta d^2}{d^2} + \frac{\Delta d^3}{d^3}\right). \tag{3.3}
 \end{aligned}$$

If we set $P_c = 5$ watts, $d = 9$ mil, $\Delta d = 1$, then substituting these into equation (3.3) we have:

$$P_c' = 6.85 \text{ watts.}$$

It can be seen that minute manufacturing tolerances have tremendous effect on the threshold power.

3. Preliminary analysis of the characteristics of an electronic multipacting limiter.

Reference [7] has given the typical characteristics of an X-band electronic multipacting limiter; we list them in the following:

peak power	250 kW
average power	3 kW
insertion loss	0.4 - 0.5 dB
recovery time	less than 5 ns
spike energy	0.2 erg max.
flat leakage	8 watts
operating life span	10,000 hours
dimensions	6" x 4" x 2.4"
weight	2.5 lbs.

It can be seen from the above data that the electronic multipacting limiter has a set of important characteristics:

capacity for high power, extremely short recovery time, broad dynamic range, small insertion loss, small volume, light weight and long operating life. Besides, since its high frequency circuit is basically a band pass filter, therefore it possesses capability to resist jamming. When an electronic multipacting limiter is operating, neither does it need arc (receiver) protecting voltage nor does it need synchronous pulse stream, therefore it is directly excited by the incoming RF waves. It is exactly due to this valuable characteristic that it is successfully applied to the high power pulse doppler radars.

We give some theoretical verification of some main characteristics of electronic multipacting limitations in the following. Since the electronic process in the limiting gap is very complex, we can therefore only make some analysis using some very simple models; however, the obtained results will at least yield some definite interpretation.

A. Computations of the time to establish electronic multipacting process

Let A and B be the two electrode plates of a limiting gap, and they are both coated with secondary emission material. The limiting gap distance is d and each electrode plate has width W . The coordinate system is set up in the following manner: x is the direction along the distance of the limiting gap, y is the direction along the width of the electrode plate, and z is the direction of the longitude of the limiting gap, as seen in Figure 3.4. Note that the high frequency energy is transmitted along the z -axis.

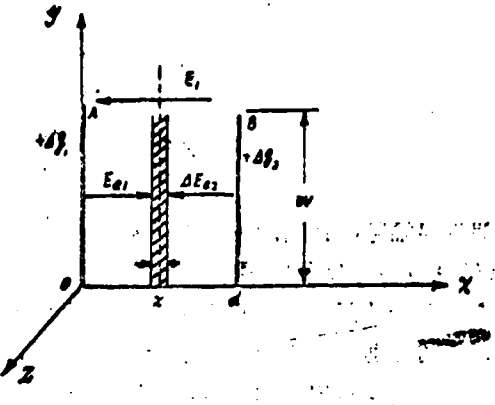


Figure 3.4.

The amplitude of the incoming high power frequency is P_1 and the amplitude of the high frequency field, set up in the limiting gap, is E_m . If E_m is greater than E_0 , the amplitude of the triggered synchronous field of the electronic multipacting process, and if primary electrons exist and

the emission coefficient σ of the secondary electrons on the electrode plates is greater than 1, the electronic multipacting process is produced.

Since the secondary emission coefficient σ of the electronic plates A and B is greater than 1, then the number of electrons emitted by the electrode plate increases by σ times as each half period is passed; this is a cascade process. On the bombarded surface of the electrode plate at a certain instant when the increase in the field set up by the space charges reaches the stage that it just cancels out the high frequency field, the number of secondary emission electrons will not increase. Then the number of the electrons which are injected by the space charges onto the electrode plates will be complemented by an equivalent number of secondary electrons emitted by the electrode plates, the dynamic

equilibrium of the quantity of the space charges of the gap is maintained, and the electronic multipacting process has entered a state of equilibrium.

We call the period of the electronic multipacting process, from the initiation of excitation to the beginning of stability, the limiter building (set up) time, and denote it by τ_A^t . Clearly, it is only necessary to compute the number of times that the electrons have multiplied in the period from excitation to stability to obtain τ_A^t .

While in the stable state the space charge is $-q$ in the unit length of the limiting gap. At x of the limiting gap, Δx is the thickness of the thin layer of charge ^{to} leave the $y-z$ plane. Its value is $-\Delta q$. Then the space charge fields on the two sides of the thin layer are respectively

$$\Delta E_{\epsilon_1} = \frac{\Delta q_1}{\epsilon_0 s}$$

$$\Delta E_{\epsilon_2} = -\frac{\Delta q_2}{\epsilon_0 s} \quad (3.4)$$

where $s = l \times W$ is the area of the unit length of the limiting gap electrode plate, and Δq_1 and Δq_2 are the respective induced charge of electroplates A and B, as shown in Figure 3.4.

According to the principle of charge conservation and considering the potential between plates A and B we leave

$$\Delta q_1 + \Delta q_2 - \Delta q = 0$$

$$\Delta E_{\epsilon_1}x + \Delta E_{\epsilon_2}(d-x) = 0$$

Solving those two equations simultaneously, we have

$$\begin{aligned}\Delta q_1 &= \Delta q \left(1 - \frac{x}{d}\right) \\ \Delta q_2 &= \Delta q - \frac{x}{d} \end{aligned}\quad (3.5)$$

Then we have

$$\begin{aligned}\Delta E_{e1} &= \frac{\Delta q}{\epsilon_0 s} \left(1 - \frac{x}{d}\right) \\ \Delta E_{e2} &= -\frac{\Delta q}{\epsilon_0 s} - \frac{x}{d} \end{aligned}\quad (3.6)$$

Suppose that initially the density of the primary electrons of the limiting gap is ρ , then the sum of the primary electrons (assuming uniform distribution) in the volume along the limiting gap unit length is $\rho s d$. Since $\sigma > 1$, after n multiplications (multipacting), the electronic multipacting process will have achieved stable state. Simultaneously considered is that under the usual working condition of the limiter, the input power far exceeds the threshold power of the triggered multipacting process. Therefore the traverse angle of motion in the gap is much smaller (minute in comparison) than the traverse angle π under the threshold power. When the traverse angle is very small the motion of the electrons in the gap may be thought of as non-congregating. Therefore, the space charges along the x-axis in stable state are uniformly distributed.

Then under equilibrium, the number of space charges in the volume along the unit length of the limiting gap is

$$q = e \rho \sigma^n s d \quad (3.7)$$

where e is the voltage of the electron.

However, the number of space charges in the volume of the thin layer, of thickness dx , in the gap is

$$dq = \epsilon_0 \sigma^* s dx$$

Therefore, under stable state, at any selected point on the x-axis but on a cross-section perpendicular to x-axis, the (space charge) field produced by the space charges in the gap should be

$$\begin{aligned} E_s(x) &= \int_0^x dE_{s1} + \int_x^d dE_{s2} \\ &= -\frac{1}{\epsilon_0 s} \int_0^x \frac{\xi}{d} dq + \frac{1}{\epsilon_0 s} \int_x^d \left(1 - \frac{\xi}{d}\right) dq \\ &= \frac{1}{\epsilon_0} \epsilon \rho \sigma^* \left[\int_x^d \left(1 - \frac{\xi}{d}\right) d\xi - \int_0^x \frac{\xi}{d} d\xi \right] \\ &= \frac{1}{\epsilon_0} \epsilon \rho \sigma^* \left(\frac{d}{2} - x \right) \end{aligned} \quad (3.8)$$

It can be seen that as $x \rightarrow 0$, the space charge field of the surface of the electroplate A is

$$E_s(0) = -\frac{1}{2\epsilon_0} \epsilon \rho \sigma^* d \quad (3.9)$$

When $x \rightarrow d$ the space charge field of plate B is

$$E_s = -\frac{1}{2\epsilon_0} \epsilon \rho \sigma^* d \quad (3.10)$$

On the cross-section at the middle of the gap, i.e., where $x = \frac{d}{2}$, the space charge field is zero. The distribution in the gap is such that it is strong on the two sides and weak in the middle.

Clearly the space charge field has a repelling effect on the secondary electrons emitted by electrode plates A and B. When the input power is greater than the threshold power, the plates A and B will alternatively emit secondary electrons with the high frequency field in synchronous fashion. The high frequency electric field has an accelerating effect on the emission of secondary electrons of plates A and B. Therefore, the relative strength of the high frequency field to the space charge field will determine the strength of the secondary emission by the electrode plate that was bombarded.

On the electrode plate surface, if

$$E_m > E_s(x) \Big|_{x \rightarrow d}^{x \rightarrow 0}$$

then the number of the emitted secondary electrons will certainly be greater than the injected primary electrons, resulting in the increase of the space charge field. This will in turn change the state of the high frequency (electric) field being greater than the space charge field. If

$$E_m < E_s(x) \Big|_{x \rightarrow d}^{x \rightarrow 0}$$

then the number of the emitted secondary electrons will certainly be less than the injected primary electrons, resulting in the decrease of the space charge field. This then will again alter the state of the high frequency field being weaker than the space charge field.

Neither one of the above two states is stable. Therefore, the only stable state exists when

$$E_m = E_s(x) \Big|_{x \rightarrow d}^{x \rightarrow 0}.$$

At this point, the number of the emitted secondary electrons is statistically equal to that of the injected primary electrons, and the space charge equilibrium state is maintained.

Then, in the stable state, on the bombarded surface of the electrode plate, we have

$$\frac{1}{2\epsilon_0} \epsilon \rho \sigma^* d = E_m$$

e.g.

$$\sigma^* = \frac{2\epsilon_0 E_m}{\epsilon \rho d} \quad (3.11)$$

Therefore, in the electronic multipacting process from the excitation to stability, the multiplication factor n may be derived from

$$n = \left[\frac{1}{\lg \sigma} \cdot \lg \left(\frac{2\epsilon_0 E_m}{\epsilon \rho d} \right) \right] \quad (3.12)$$

Where [] denote the integer function, i.e. taking only the integer part of the number.

Since it requires one-half of a high frequency period to achieve one multiplication, the time, τ_A , it takes for the electronic multipacting to occur is

$$\tau_A = \frac{1}{2f} \left[\frac{1}{\lg \sigma} \cdot \lg \left(\frac{2\epsilon_0 E_m}{\epsilon \rho d} \right) \right] \quad (3.13)$$

Set $d = 9$ mils, $W = 8$ mm, $P_1 = 200$ kW, $\delta = 10$, $p = 100/(mm)^3$, $f = 10$ GHz; substituting into equation (3.13), we have

$$\tau_A \approx 0.55 \text{ nanoseconds}$$

It can be seen that the past-motion process of the electronic multipacting limiter is very short. Clearly, from the above computations, we have actually hypothesized the emitting frequency pulse is ideally a rectangular pulse. The actual emitting frequency pulses always have a forward course. Suppose that the forward course rise time is τ_f ; when $\tau_f < \tau_A$, the setup time for the electronic multipacting process is τ_A , as obtained above. When $\tau_f > \tau_A$, due to the fact that the electronic multipacting process is limited by the forward course of the pulses, the setup time is essentially equal to τ_f .

B. The computation of the recovery time

After the electronic multipacting process has entered a stable state, if the emitting power of the input limiting gap is suddenly terminated, the electronic multipacting process is terminated as well. Even though the multipacting process of the electrons is terminated, the space charges already exist within the limiting gap, i.e., it takes a certain length of time for them (the space charges) to completely dissipate from the external field. We take the period of time from the termination in the external field to the complete dissipation of the space charges to be τ_B , the recovery time for the electronic multipacting limiter.

How is this time computed? Clearly, when the external field is terminated, the electrons on the different cross-sections of the gap, due to the spatial relationship and motion states, are all different. Therefore, the times required for the space charges to dissipate completely and their motion are all different. We take only the longest time to be typical in the computation, and take the time from its termination in the external field to that required

for the motion, under the influence of the space charge field, to the electrode plates, and use it as the approximate recovery time.

This kind of typical electron may be chosen in the following manner: when the external field is suddenly terminated, it has just left the surface of the bombarded electrode plate. Also, suppose that this kind of electron has, while leaving the emitting surface, absorbed the bombarding energy of a primary electron. Then its initial velocity is not zero.

Let K be the absorption coefficient of the energy of the absorbed primary electron, and let v_0 be the initial velocity of the electron when it leaves the electrode plate. Then

$$v_0 = \sqrt{2K\eta d E_\infty}$$

where $\eta = \frac{e}{m}$ is the charge ratio of the electron.

The kinetic equation of the electron, in the limiting gap, under the influence of the space charge field is

$$m\ddot{x} = eE_\infty(x). \quad (3.15)$$

Substituting (3.8) and (3.11) into equation (3.15), and simplifying, we obtain

$$\ddot{x} - \frac{2E_\infty\eta}{d}x + \eta E_\infty = 0. \quad (3.16)$$

Its general solution is

$$x = \frac{d}{2} + c_1 e^{rt} + c_2 e^{-rt}$$

where $r = \sqrt{\frac{2\eta E_m}{d}}$.

When $t = 0$ and $x = 0$, we have

$$0 = -\frac{d}{2} + c_1 + c_2$$

When $t = 0$ and $x = v_0$, we have

$$v_0 = c_1 r - c_2 r$$

from which we can ascertain that

$$c_1 = \frac{1}{2} \left(\frac{v_0}{r} - \frac{d}{2} \right)$$

$$c_2 = \frac{1}{2} \left(\frac{v_0}{r} + \frac{d}{2} \right).$$

Substituting c_1 and c_2 into the general solution of the equation, we get

$$\begin{aligned} x &= \frac{d}{2} + \frac{1}{2} \left(\frac{v_0}{r} - \frac{d}{2} \right) e^{rt} - \frac{1}{2} \left(\frac{v_0}{r} + \frac{d}{2} \right) e^{-rt} \\ &= \frac{d}{2} + \frac{v_0}{r} \sin(rt) - \frac{d}{2} \cosh(rt). \end{aligned} \quad (3.17)$$

Set $x = d$, then $t = \tau_B$, and we have

$$\begin{aligned} d &= \frac{d}{2} + \frac{v_0}{r} \sin(r\tau_B) - \frac{d}{2} \cosh(r\tau_B) \\ d &= \frac{2v_0}{r} \sin(r\tau_B) - d \cosh(r\tau_B) \end{aligned}$$

$$d[1 + \operatorname{ch}(\frac{r\tau_B}{2})] = \frac{2v_0}{r} \operatorname{sh}(\frac{r\tau_B}{2})$$

$$d[1 + \operatorname{ch}^2(\frac{r\tau_B}{2}) + \operatorname{sh}^2(\frac{r\tau_B}{2})] = \frac{2v_0}{r} + 2\operatorname{sh}(\frac{r\tau_B}{2})\operatorname{ch}(\frac{r\tau_B}{2})$$

$$\operatorname{ch}^2(\frac{r\tau_B}{2}) = \frac{2v_0}{rd} \operatorname{sh}(\frac{r\tau_B}{2})\operatorname{ch}(\frac{r\tau_B}{2})$$

Since $\operatorname{ch}(\frac{r\tau_B}{2}) \neq 0$, dividing both sides of the above equation by $\operatorname{ch}^2(\frac{r\tau_B}{2})$ we have

$$\operatorname{th}(\frac{r\tau_B}{2}) = \frac{rd}{2v_0}$$

Therefore,

$$\begin{aligned} \tau_B &= -\frac{2}{r} \operatorname{th}^{-1}\left(\frac{rd}{2v_0}\right) \\ &= -\frac{1}{r} \ln \frac{1 + \frac{rd}{2v_0}}{1 - \frac{rd}{2v_0}} \\ &= \frac{1}{r} \ln \frac{2v_0 + rd}{2v_0 - rd} \end{aligned} \quad (3.18)$$

$$r = \sqrt{\frac{2\eta E_m}{d}}$$

(3.18)
We finally arrive at

$$\tau_B = \sqrt{\frac{d}{2\eta E_m}} \ln \frac{2\sqrt{K} + 1}{2\sqrt{K} - 1} \quad (3.19)$$

Clearly, we can see from (3.19) that only when $K > 1/4$ does above equation have any physical meaning. It shows that only those secondary electrons which had absorbed more than 25% of the bombarding energy of the primary electrons can, after the termination of the external field, overcome the repelling force of the space charge field, to arrive in the next (facing)

electrode plate. Those electrons which have not achieved this energy level will fall back to their original position.

In the above computations we treated the space charge field as time invariant. Of course, this introduces bias into the results of our computations. Actually, when the external field is terminated the space charge field is dissipated along with it, i.e., the space charge field gradually diminishes. However, the distribution of the space charge field along the x-axis is such that it is strong at the two ends but weak in the middle, but the distribution in the high frequency field is homogeneous. Therefore, the bias value in the space charge field induces an effect on the kinetic state of the electronic dissipation process. This is small compared to the initial kinetic state of the electrons, determined by the high frequency field. So, in the dissipation process of the electrons the space charge field is viewed as being time invariant. The computed recovery time under such an assumption will not have large bias.

It can be thus seen that the duration (length) of the recovery time mainly depends on the strength (intensity) of the high frequency field. The stronger the high frequency field, the shorter the recovery time.

Let $P_1 = 10$ watts, $d = 9$ mils, $W = 8$ mm, $K = 0.5$,
then $\tau_B \approx 0.2$ nsec.

It can be seen from the results of the computation that the electronic multipacting limiter recovery time is in the range of nanoseconds. Therefore, it can better satisfy the requirements of the pulse doppler radars.

C. Computation of flat leakage

After the electronic multipacting process has entered the stable condition, the width of the limiting gap is 1, the electronic cloud has absorbed the vast majority of the input power, and the remaining (input power) is expressed as flat leakage, denoted by P_f .

We introduce the attenuating constant β to express the absorption effect of the electronic cloud. It can be proved that β is merely a constant, and is not related to the coordinate Z .

Therefore, on one hand, we may view from the attenuation of transmission, and the flat leakage power P_f may be expressed as

$$P_f = P_i e^{-\beta Z}. \quad (3.20)$$

On the other hand, we may derive the absorption power P_e of the electronic cloud, from the physical process of the produced attenuation, and P_f may be expressed also as

$$P_f = P_i - P_e. \quad (3.21)$$

We know, from the absorption effect of the electronic cloud, that the high frequency field along the longitudinal direction of the limiting gap is attenuating, and it can be expressed by

$$E_m(Z) = E_m e^{-\beta Z}. \quad (3.22)$$

Therefore, the space charge density along the Z -axis is non-homogeneous. We know from equations (3.7) and (3.11) the small volume $Wd\Delta Z$, covering some point Z on the length of the

limiting gap, contains space charges of quantity

$$\Delta q = 2\epsilon_0 W E_m e^{-\beta Z} \Delta Z.$$

These space charges, under the effect of high frequency field, have the respective absorbing high frequency field energy and average power, from one electrode plate to another in the limiting gap,

$$\begin{aligned}\Delta W_s &= \Delta q E_m(Z) d \\ &= 2\epsilon_0 W d E_m^2 e^{-\beta Z} \Delta Z \\ \Delta P_s &= \frac{\Delta W_s}{T} \\ &= 4\epsilon_0 W d f E_m^2 e^{-\beta Z} \Delta Z.\end{aligned}$$

The power absorbed by the entire spectrum of the electronic cloud in the limiting gap is

$$P_s = \int_0^l dP_s$$

$$= 2\epsilon_0 W d f E_m^2 \frac{1 - e^{-2\beta l}}{\beta}. \quad (3.23)$$

Therefore,

$$P_i = P_s - 2\epsilon_0 W d f E_m^2 \frac{1 - e^{-2\beta l}}{\beta}. \quad (3.24)$$

Then, from equations (3.20) and (3.24) we obtain

$$\beta = \frac{2\epsilon_0 W d f E_m^2}{P_i}. \quad (3.25)$$

Therefore, we may obtain the flat leakage power by substituting the value of β , as in equation (3.25), into equation (3.20).

Furthermore, from the condition $P_f = P_c$, we may determine the maximum value of the limiting gap.

$$l_{\max} = \frac{1}{2\beta} \ln \frac{P_f}{P_c}. \quad (3.26)$$

Let $P_i = 200$ ~~kw~~ $P_e = 5W$, $f = 10$ GHz, $d = 9$ mils, $W = 8$ mm, substituting these into equations (3.25) and (3.26) we get

$$l_{\max} \approx 4.1 \text{ cm.}$$

Clearly, the dimensions of the electronic multipacting limiter are not large.

If we substitute the l_{\max} of equation (3.26) into equation (3.20), clearly, the flat leakage thus obtained is the least, i.e.

$$(P_f)_{\text{flat}} = P_c$$

Therefore, we may use the requirements of P_f to generally determine the length l of the limiting gap. Clearly, the value of l will not exceed l_{\max} , otherwise reducing the flat leakage would not have practical meaning.

D. The computation of peak energy

Peak energy pertains to the total emitting frequency energy which leaks through the limiting gap, in the entire set up process, while the input power is being transmitted through the limiter.

Clearly, if the emitting pulses had not moved forward,

even though the set up time for the electronic multipacting limiter is very short, the peak energy is still very large. In reality the pulses will certainly move forward. We only make computations and analysis, under the assumption that the time it takes the pulses to move forward is larger than τ_A in the following.

Under normal conditions the length covered by the forward motion of the pulses does not increase as fast as the electronic multipacting. Therefore, when we consider the effect of the lengthening of the pulses, we must take into account the fact that the increase of space charges in the gap of the set up process will no longer obey the exponent law but the rule on the lengthening forward motion of the emitting pulses. Under such conditions, the quantity of the space charges in the gap, at any instant t , is determined by the quantity of the input power of that instant. Therefore, during the set up process in every instant of time the electronic process may be viewed as a kind of quasi-stable process. Then, we may directly use in the following analysis some relations derived in the stable state, i.e., we need only consider the effect of the factors which are unique during the quasi-stable process.

When we consider the forward motion of the pulses the input emitting power may be expressed as

$$P_i(t) = P_i \left(1 - e^{-\frac{t}{T_0}}\right)^2$$

where T_0 is a constant related to the circuit formed by pulses.

According to (3.20) and (3.21) the instantaneous power absorbed by the electronic cloud in the gap is

$$p_e(t) = p_e (1 - e^{-\frac{t}{T_0}}) (1 - e^{-\frac{t}{T_0}})^2.$$

Therefore, the instantaneous power which leaks through the limiting gap during the instant t is equal to

$$P_i(t) = P_i \left(1 - e^{-\frac{t}{T_0}}\right)^2 + P_i \left(1 - e^{-2Bt}\right) \left(1 - e^{-\frac{t}{T_0}}\right)^2. \quad (3.27)$$

Integrating equation (3.27), we can obtain the peak spike energy

$$\begin{aligned} W_s &= P_i \int_0^{\tau_f} \left(1 - e^{-\frac{t}{T_0}}\right)^2 dt + P_i \left(1 - e^{-2B\tau_f}\right) \int_{\tau_c}^{\tau_f} \left(1 - e^{-\frac{t}{T_0}}\right)^2 dt \\ &= P_i \left\{ \left[\tau_c - 2T_0 \left(1 - e^{-\frac{\tau_c}{T_0}}\right) + \frac{T_0}{2} \left(1 - e^{-\frac{2\tau_c}{T_0}}\right) \right] \right. \\ &\quad \left. + e^{-2B\tau_f} \left[(\tau_f - \tau_c) - 2T_0 \left(e^{-\frac{\tau_c}{T_0}} - e^{-\frac{\tau_f}{T_0}}\right) + \frac{T_0}{2} \left(e^{-\frac{2\tau_c}{T_0}} - e^{-\frac{2\tau_f}{T_0}}\right) \right] \right\} \quad (3.28) \end{aligned}$$

where τ_f is the set up time of the pulses in the forward movement set up process, τ_c is the corresponding time it takes for the forward moving pulses to rise to the peak value P_c .

Let $P_i = 200$ KW, $\tau_f = 0.03$ msec, and T_0 is determined by the relation

$$0.9E_m = E_m \left(1 - e^{-\frac{\tau_f}{T_0}}\right)$$

where $e^{-\frac{\tau_f}{T_0}} = 0.1$.

τ_c is determined by the relation

$$P_i \left(1 - e^{-\frac{\tau_c}{T_0}}\right)^2 = P_c$$

where $e - \frac{\tau c}{T_0} = 0.995$.

Substituting these into equation (3.28) we finally arrive at the peak spike energy

$$W_s \approx 0.65 \text{ erg.}$$

If we calculate according to the width of 3 dB wave peak the peak spike energy (value) will be even smaller.

We can see from computations of several characteristic parameters in the above that the recovery time of the electronic multipacting limiter is extremely short however, the flat leakage and the peak spike energy are not small enough. Therefore, in applications we still need to append a solid diode limiter behind the electronic multipacting limiter, in order to sufficiently protect the receiver, as shown in Figure 3.3.

CONCLUSIONS

This paper has given discussions of three types of limiters: ferrite-diode limiter, plasma limiter, and electronic multipacting limiter. Each can be viewed being applicable in the field of high power, high pulse repetition frequency (PRF), doppler radars, and each type possesses its own characteristics. From the comprehensive point of view the electronic multipacting limiter is currently the best. This paper has derived the necessary equations for reference in design and research. Since the threshold power of the electronic multipacting process is directly proportional to the cube of the limiting gap (distance), therefore, stringent tolerance must be maintained in the control of the limiting gap; this introduces a very difficult problem into the study of this kind of device. Furthermore, more research needs to be conducted on the bandwidth of this kind of device.

Finally, we gratefully acknowledge the tremendous support and assistance rendered us by Wan Ren-Dau, Chief Engineer of No. 4404 Factory, and Comrade He Jin-Sun of the Institute of Electronics, Chinese Academy of Sciences.

REFERENCES

- [1] Microwave Journal, February 1974, pp. 6-66.
- [2] Microwave Journal, Dec. 1973, pp. 53-57.
- [3] IEEE Trans. MTT-18, No. 9, 1970, pp. 652-654.
- [4] Proc. IRE, Vol. 44, No. 10, 1956, pp. 1270-1284.
- [5] IEEE Trans. MTT-20, No. 2, 1972, pp. 193-194.
- [6] Microwave, Jan. 1976, pp. 57-60.
- [7] Microwave, July, 1974, pp. 52-53.
- [8] Journal of Applied Physics, Vol. 32, No. 6, 1961, p. 1086.

ANALYSES OF HIGH-POWER RADAR TA-LIMITER WITH VERY SHORT RECOVERY TIME

Hsu Jun-min Tong Cin-shian

ABSTRACT

This paper describes three types of high-power radar *TR*-limiter with short recovery time. These devices are plasma-diode, ferrite-diode and multipactor limiter. The last one is analysed in detail, which will give aid to design of this device.